HUMAN HEAD - NECK SYSTEM: THE EFFECT OF VISCOELASTIC NECK ON THE EIGENFREQUENCY SPECTRUM

A. Charalambopoulos, D.I. Fotiadis and C.V. Massalas

18-97

Preprint no. 18-97/1997

Department of Computer Science
University of Ioannina
451 10 Ioannina, Greece

HUMAN HEAD - NECK SYSTEM: THE EFFECT OF VISCOELASTIC NECK ON THE EIGENFREQUENCY SPECTRUM

A. CHARALAMBOPOULOS

Polytechnic School, Mathematics Division, Aristotle University of Thessaloniki, GR 540 06 Thessaloniki, Greece

D.I. FOTIADIS

Dept. of Computer Science, Univ. of Ioannina, GR 45110 Ioannina, Greece

and

C.V. MASSALAS

Dept. of Mathematics, Univ. of Ioannina, GR 45110 Ioannina, Greece

Key Words: Human head-neck system, dynamic characteristics, neck viscoelasticity.

Abstract

The present study is concerned with the determination of the dynamic characteristics of the human head - neck system which is described by a fluid filled spherical cavity supported by a viscoelastic neck which reacts in three dimensions. The material of the skull is assumed to be a homogeneous, isotropic, elastic material and that of the brain - cerebrospinal fluid an inviscid irrotational fluid. The neck is approximated by a three element elastic model the constants of which are computed by using experimental data. The results obtained show that the viscoelastic properties of the neck affect only the first two eigenfrequencies and the corresponding damping coefficients while the remaining spectrum remains unchanged.

1. Introduction

In a previous communication [1] we have presented a model of the human head - neck system in which the neck is approximated by elastic strings acting in three dimensions. We have understood that the neck support plays an important role on the eigenfrequency spectrum of the system. It introduces a shifting of the spectrum and two new eigefrequencies which are the smallest ones for the system. Håkansson et al. [2] have presented a comprehensive investigation of the resonance frequencies of the human skull *in vivo*. Their findings include measurements of the system frequencies as well as damping coefficients. We have recently developed models which take into account the viscoelastic behavior of the human skull and brain [3-4] using properties which have been reported previously by other researchers [5-6]. We obtained good agreement with the experimentally reported eigenfrequencies but discrepancies observed between our results and those reported in Ref. 2 for the damping coefficients. One of the reasons might be the ignorance of the neck viscoelastic behavior.

Landkof et al. [7] presented an analytical and experimental study involving non - destructive, axisymmetric impact on a fluid - filled constrained by a viscoelastic, artificial neck. The constants of the viscoelastic model proposed were determined by fitting data using least squares. Misra et al. [8] included in the study of the head - neck system a viscoelastic neck support. They considered elastic, homogeneous and isotropic skull, while the brain was regarded as inviscid and compressible fluid with its motion irrotational. The artificial neck was represented analytically by a linear viscoelastic cantilever beam that was rigidly connected to the skull.

Because of the importance of the system motion in head injury other researchers have proposed models for the same system. Reber and Goldsmith [9] have developed a two dimensional model to predict the motion under impact loadings and upper torso

accelerations. Later Merill et al. [10] extended the model to a three dimensional one. However, to our knowledge no other attempt has been reported on the predictions of the frequency characteristics of the human head - neck system. Those dynamic characteristics are useful in determining brain diseases through a semi - interference method which is based on the shifting of eigenfrequencies spectrum. The process is related to the intracranial pressure - volume relationship attributed to Langfitt et al. [11]. Such a method can be proved operative if according to experimental observations sudden changes in intracranial pressure have a measurable relative effect on the frequencies spectrum with or without the use of a protective helmet, the later have discussed by other researchers [12].

In this work we perform an analysis of the frequency spectrum of the human head - neck system. The human skull is simulated by a linear, isotropic, homogeneous, elastic material. The brain is supposed to be an inviscid irrotational incompressible fluid undergoing small oscillations, since we have observed that the effect of viscoelasticity is small for resonance frequencies [4]. The cerebrospinal fluid is treated in the same way. Finally, the neck support is approximated by a three - element model which reacts in three dimensions. The mathematical model is based on the three - dimensional theory of elasticity and the representation of the displacement fields in terms of the Navier eigenvectors [13]. The coefficients involved in the three element elastic model for the neck support are determined by the existing experimental data. Those coefficients are used for the computations of the eigenfrequency spectrum. In addition, a model for the neck is described. The spectrum is computed for several parameters involved in the model which correspond to real human head cases. The results obtained show good agreement with experimental data both for the eigenfrequency and damping coefficients. However, it is not possible to predict the first eigenfrequency. Further study which includes other characteristics not described by our model might give a better insight of the first eigenfrequency behavior.

2. Problem Formulation

The system under consideration is presented in Figure 1. It consists of an elastic sphere (1 - skull) containing an inviscid and irrotational fluid material (0 - brain/cerebrospinal fluid) while the whole structure is supported by the viscoelastic neck whose simulation in the model is realised through a particular type of boundary conditions imposed on S_1. The boundary conditions have to involve the geometric as well as the physical characteristics of the neck support mechanism.

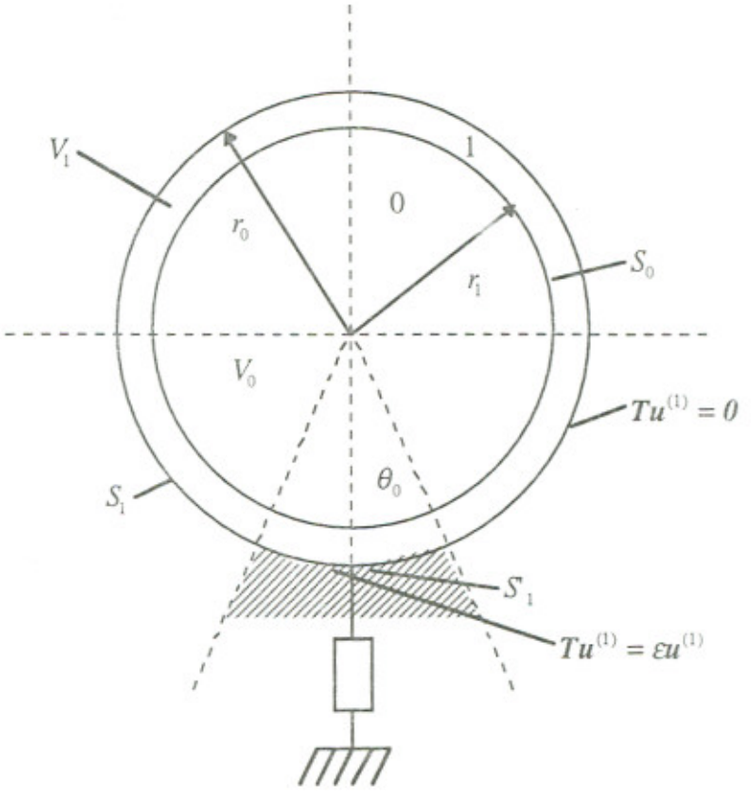

Figure 1: Problem Geometry.

The aim of this work is the determination of the dynamic characteristics of the above system, that is its natural frequencies and the corresponding attenuation coefficients due to the viscoelastic character of the neck.

The material of the region 1 is characterised completely by Lamè's constants λ and μ and the mass density ρ_1. Its motion is fully described by the displacement field $\boldsymbol{u}^{(1)}(\boldsymbol{r},t)$, which satisfies the elasticity equation

$$\mu\nabla^2\boldsymbol{u}^{(1)}(\boldsymbol{r},t)+(\lambda+\mu)\nabla(\nabla\cdot\boldsymbol{u}^{(1)}(\boldsymbol{r},t))=\rho_1\frac{\partial^2\boldsymbol{u}^{(1)}(\boldsymbol{r},t)}{\partial t^2}, \tag{1}$$

where ∇ is the del - operator and t is the time.

The motion of region - 0 is studied after making the assumption that the inviscid and irrotational fluid occupying this region undergoes small oscillations. Then its motion is governed by the wave equation

$$\nabla^2\Phi(\boldsymbol{r},t)=\frac{1}{c_f^2}\frac{\partial^2\Phi(\boldsymbol{r},t)}{\partial t^2}\ , \tag{2}$$

where $\Phi(\boldsymbol{r},t)$ is the velocity potential and c_f is the speed of sound in the fluid.

The pressure P of the fluid can be determined from the velocity potential through the relation

$$P=-\rho_f\left(\frac{\partial\Phi}{\partial t}\right), \tag{3}$$

where ρ_f stands for the mass density of the fluid.

As it is already mentioned, the neck support mechanism creates attenuation due to its viscous properties. Consequently, postponing the introduction of viscosity until the

boundary conditions are described, we assume harmonic motion of the whole system with angular frequency ω_1 and attenuation ω_2.

We apply then Fourier transform analysis to the problem defining

$$\hat{u}^{(1)}(r,\omega) = \int_{-\infty}^{+\infty} u^{(1)}(r,t)e^{+i\omega t}dt \tag{4}$$

$$\hat{\Phi}(r,\omega) = \int_{-\infty}^{+\infty} \Phi(r,t)e^{+i\omega t}dt \tag{5}$$

$$\hat{P}(r,\omega) = \int_{-\infty}^{+\infty} P(r,t)e^{+i\omega t}dt \tag{6}$$

with $\omega = \omega_1 + i\omega_2$ $(i = \sqrt{-1})$.

For simplicity, we suppress the dependence of previous transformed functions on their argument ω.

Taking advantage of the Fourier transform properties the equations (1), (2), (3) lead to the following equations concerning now the functions $\boldsymbol{u}^{(1)}(\boldsymbol{r})$, $\hat{\Phi}(\boldsymbol{r})$, $\hat{P}(\boldsymbol{r})$,

$$\mu\nabla^2\hat{u}(r) + (\lambda+\mu)\nabla(\nabla\cdot\hat{u}^{(1)}(r)) + \rho_1\omega^2\hat{u}^{(1)}(r) = 0 \tag{7}$$

$$\nabla^2\hat{\Phi}(r) + k_f^2\hat{\Phi}(r) = 0 \tag{8}$$

$$\hat{P}(r) = i\omega\rho_f\hat{\Phi}(r) \tag{9}$$

where $k_f = \frac{\omega}{c_f}$.

In order to study the dynamic properties of the system in a uniform manner we introduce dimensionless variables.

More precisely, evoking the velocities $c_p = \sqrt{(\lambda + 2\mu)/\rho_1}$, $c_s = \sqrt{\mu/\rho_1}$, which describe completely the elastic medium - 1 alternatively to Lamè's constants, we define the following dimensionless quantities

$$r' = \frac{r}{\alpha}, \quad \Omega = \frac{\omega\alpha}{c_p} \quad (\alpha = r_2)$$

$$\nabla' = \alpha\nabla, \; c'_s = \frac{c_s}{c_p}, \; c'_p = 1, \; c'_f = \frac{c_f}{c_{p_2}}, \; k'_f = \frac{\Omega}{c_f}, \; \rho'_f = \frac{\rho_f}{\rho_1}.$$

The differential equations (1) and (2) in dimensionless form are written as

$$c'^2_s \nabla'^2 \hat{\boldsymbol{u}}^{(1)}(\boldsymbol{r}') + (c'^2_p - c'^2_s)\nabla'(\nabla' \cdot \hat{\boldsymbol{u}}^{(1)}(\boldsymbol{r}')) + \Omega^2 \hat{\boldsymbol{u}}^{(1)}(\boldsymbol{r}') = \boldsymbol{0} \tag{10}$$

$$\nabla'^2 \hat{\Phi}(\boldsymbol{r}') + k'^2_f \hat{\Phi}(\boldsymbol{r}') = 0. \tag{11}$$

The pressure $\hat{P}$ in dimensionless form is given by

$$\hat{P}(\boldsymbol{r}') = i\Omega\rho'_f \frac{1}{c'^2_s}\hat{\Phi}(\boldsymbol{r}'). \tag{12}$$

As we have already mentioned, the velocity potential $\hat{\Phi}(\boldsymbol{r}')$ is the fundamental quantity in terms of which all the useful quantities characterising the motion of the fluid occupying region - 0 can be expressed.

So, we introduce here the fluid velocity $\hat{v}(r')$ and the displacement field $\hat{u}^{(0)}(r')$ in dimensionless form as follows

$$\hat{v}(r') = \nabla' \Phi(r') \tag{13}$$

$$\hat{u}^{(0)}(r') = \frac{i}{\Omega}\hat{v}(r'). \tag{14}$$

The displacement fields $\hat{u}^{(0)}$, $\hat{u}^{(1)}$ and the pressure $\hat{P}$, in addition to equations (10), (11), (12), (14) satisfy the boundary conditions expressing the interaction of the partial components of the system.

As far as the surface S_0 is concerned, we have the continuity of the displacement fields, while the stress field due to the elastic medium must be compensated by the pressure of the fluid, that is

$$\hat{u}^{(1)}(r') = \hat{u}^{(0)}(r'), \quad r' \in S_0, \tag{15}$$

$$T'\hat{u}^{(0)}(r') = -\hat{P}(r')\hat{r}, \quad r' \in S_0 \tag{16}$$

where

$$T' = 2\mu'\hat{r}\cdot\nabla' + \lambda'\hat{r}\times(\nabla'\cdot) + \mu'\hat{r}\times(\nabla'\times) \tag{17}$$

stands for the dimensionless surface stress operator on S_0, $\hat{r}$ is the unit outward normal vector on S_0 and $(\lambda', \mu') = \left(\frac{\lambda}{\mu}, \frac{\mu}{\mu}\right) = \left(\frac{\lambda}{\mu}, 1\right)$.

The boundary conditions satisfied by the elastic field on the exterior surface S_1 is of mixed type. More precisely, the surface section shown in Fig. 1 in the region

$0 \le \vartheta < \pi - \theta_0$ is stress free, while the surface section $\pi - \theta_0 \le \vartheta \le \pi$ represents the neck support and the boundary condition satisfied there must incorporate the physical character of the interaction between human head and neck. We assume that a Robin type boundary condition is satisfied, which simulates appropriately the dynamic character of the motion of the contact region.

The boundary condition on surface S_1 is described by

$$T\hat{u}^{(1)}(r') = \begin{cases} 0, & 0 \le \vartheta < \pi - \theta_0, \quad r' \in (S_1 \setminus S_1) \\ \varepsilon \hat{u}^{(1)}(r'), & \pi - \theta_0 \le \vartheta \le \pi, \quad r' \in S_1 \end{cases} \tag{18}$$

where $\varepsilon = \varepsilon_1 + i\varepsilon_2$ is the crucial parameter incorporating the physical characteristics of the human neck. In contrast to our previous work [1], the parameter ε has a non-zero imaginary part due to the viscous properties of the neck. This term is responsible for the damping of the system. Although only this term carries on the viscoelastic behavior of the system, the treatment of the problem is affected drastically because of the assumption of complex eigenfrequencies, fact leading, as it will be explained in what follows, to much more difficult approach.

We note that the problem described by the equations (10), (11), (12) and the boundary conditions (15), (16) and (18) constitutes a well - posed boundary value problem.

3. Problem Solution - Frequency Equation

Adopting the methodology followed in Ref. 1 we expand the elastic displacement field $\hat{u}^{(1)}(r')$ in terms of the Navier eigenvectors [13], the velocity potential $\hat{\Phi}(r')$ in terms of the Helmholtz equation basis solutions and then, we find expansions for $\hat{u}^{0}(r')$ and $\hat{P}(r')$ via their definition relations. The above mentioned procedure leads to

$$\hat{\boldsymbol{u}}^{(1)}(\boldsymbol{r}') = \sum_{n=0}^{+\infty} \sum_{m=-n}^{n} \sum_{l=1}^{2} \left\{ \alpha_n^{m,l} \boldsymbol{L}_n^{m,l}(\boldsymbol{r}') + \beta_n^{m,l} \boldsymbol{M}_n^{m,l}(\boldsymbol{r}') + \gamma_n^{m,l} \boldsymbol{N}_n^{m,l}(\boldsymbol{r}') \right\} \tag{19}$$

$$\hat{\Phi}(r') = \sum_{n=0}^{\infty} \sum_{m=-n}^{n} \left\{ c_n^m g_n^1(k'_f r') P_n^m(\cos\vartheta) e^{im\varphi} \right\} \tag{20}$$

$$\hat{u}^{(0)}(\boldsymbol{r}') = i \sum_{n=0}^{+\infty} \sum_{m=-n}^{n} c_n^m \boldsymbol{L}_n^{m,1}(\boldsymbol{r}') \tag{21}$$

$$\hat{P}(r') = i\Omega\rho'_f \frac{1}{c'^2_s} \sum_{n=0}^{+\infty} \sum_{m=-n}^{n} \left\{ c_n^m g_n^1(k'_f r') P_n^m(\cos\vartheta) e^{im\varphi} \right\}, \tag{22}$$

where $g_n^1(z)$ and $g_n^2(z)$ represent the spherical Bessel functions of the first, $j_n(z)$, and second kind, $y_n(z)$, respectively. The functions $P_n^m(\cos\vartheta)$ are the Legendre functions and the product $P_n^m(\cos\vartheta)e^{im\varphi}$ constitutes the spherical harmonic $Y_n^m(r')$.

The Navier eigenvectors are given as

$$\boldsymbol{L}_n^{m,l}(\boldsymbol{r}') = \dot{g}_n^l(k'_p r') P_n^m(\hat{\boldsymbol{r}}) + \sqrt{n(n+1)} \frac{g_n^l(k'_p r')}{k'_p r'} \boldsymbol{B}_n^m(\hat{\boldsymbol{r}}) \tag{23}$$

$$\boldsymbol{M}_n^{m,l}(\boldsymbol{r}') = \sqrt{n(n+1)} g_n^l(k'_s r') \boldsymbol{C}_n^m(\boldsymbol{r}') \tag{24}$$

$$\boldsymbol{N}_n^{m,l}(\boldsymbol{r}') = n(n+1) \frac{g_n^l(k'_s r')}{k'_s r'} \boldsymbol{P}_n^m(\hat{\boldsymbol{r}}) + \sqrt{n(n+1)} \left\{ \dot{g}_n^l(k'_s r') + \frac{g_n^l(k'_s r')}{k'_s r'} \right\} \boldsymbol{B}_n^m(\hat{\boldsymbol{r}}) \tag{25}$$

where $\dot{g}_n^l(z)$ stands for the derivative of $g_n^l(z)$ with respect to its argument and the functions $\boldsymbol{P}_n^m(\hat{\boldsymbol{r}})$, $\boldsymbol{B}_n^m(\hat{\boldsymbol{r}})$, $\boldsymbol{C}_n^m(\hat{\boldsymbol{r}})$ constitute the vector spherical harmonics given by

$$P_n^m(\hat{r}) = \hat{r} Y_n^m(\hat{r}) \tag{26}$$

$$B_n^m(\hat{r}) = \frac{1}{\sqrt{n(n+1)}} \left\{ \hat{\vartheta} \frac{\partial}{\partial \vartheta} + \hat{\varphi} \frac{1}{\sin \vartheta} \frac{\partial}{\partial \varphi} \right\} Y_n^m(\hat{r}) \tag{27}$$

$$C_n^m(\hat{r}) = \frac{1}{\sqrt{n(n+1)}} \left\{ \hat{\vartheta} \frac{1}{\sin \vartheta} \frac{\partial}{\partial \varphi} - \hat{\varphi} \frac{\partial}{\partial \vartheta} \right\} Y_n^m(\hat{r}) \tag{28}$$

where $\hat{r}$, $\hat{\vartheta}$, $\hat{\varphi}$ are the unit vectors in r, ϑ, φ - directions respectively, $k'_p = \frac{\Omega}{c'_p}$ and $k'_s = \frac{\Omega}{c'_s}$.

Forcing the expansions (19), (21), (22) to satisfy the boundary conditions (15), (16) and (18) and following the procedure presented in [1], we find that the involved coefficients must satisfy the following relations

$$\sum_{l=1}^{2} \left[\alpha_{n'}^{m',l} A_{n'}^{l}(r'_0) + \gamma_{n'}^{m',l} D_{n'}^{l}(r'_0) \right] = -i\Omega \rho'_f \frac{1}{c'^2_s} c_{n'}^{m'} g_{n'}^{1}(k'_f r'_0) \tag{29}$$

$$\sum_{l=1}^{2} \left[\alpha_{n'}^{m',l} B_{n'}^{l}(r'_0) + \gamma_{n'}^{m',l} E_{n'}^{l}(r'_0) \right] = 0 \tag{30}$$

$$\sum_{l=1}^{2} \left[\beta_{n'}^{m',l} C_{n'}^{l}(r'_0) \right] = 0 \tag{31}$$

$$\sum_{l=1}^{2} \left[\alpha_{n'}^{m',l} \dot{g}_{n'}^{l}(\Omega r'_0) + \gamma_{n'}^{m',l} n'(n'+1) \frac{g_{n'}^{l}(k'_s r'_0)}{k'_s r'_0} \right] = i c_{n'}^{m'} \dot{g}_{n'}^{l}(k'_f r'_0) \tag{32}$$

$$\sum_{l=1}^{2} \left[\alpha_{n'}^{m',l} A_{n'}^{l}(r'_1) + \gamma_{n'}^{m',l} D_{n'}^{l}(r'_1) \right] = \sum_{n=|m'|}^{+\infty} \sum_{l=1}^{2} \left[\alpha_{n}^{m',l} \hat{A}_{n}^{l}(r'_1) + \gamma_{n}^{m',l} \hat{D}_{n}^{l}(r'_1) \right] \Xi(n', n, \theta_0, m') \tag{33}$$

$$\sum_{l=1}^{2} \left[\alpha_{n'}^{m',l} B_{n'}^{l}(r'_1) + \gamma_{n'}^{m',l} E_{n'}^{l}(r'_1) \right] = \sum_{n=|m'|}^{+\infty} \sum_{l=1}^{2} \left[\alpha_{n}^{m',l} \hat{B}_{n}^{l}(r'_1) + \gamma_{n}^{m',l} \hat{E}_{n}^{l}(r'_1) \right] \Xi_1(n', n, \theta_0, m') \tag{34}$$

and

$$\sum_{l=1}^{2} \beta_{n'}^{m',l} C_{n'}^{l}(r'_1) = \sum_{n=|m'|}^{+\infty} \sum_{l=1}^{2} \beta_{n}^{m',l} \hat{C}_{n}^{l}(r'_1) \Xi_1(n', n, \theta_0, m') \tag{35}$$

where $n' = 0,1,2,...;\ |m'| \le n'$

and

$$\Xi(n',n,\theta_0,m') = \varepsilon\sqrt{\pi}\sum_{\substack{i=|n'-n| \\ i-n'+n=\text{even}}}^{n+n'} \left\{ \begin{array}{l} \dfrac{\sqrt{2i+1}}{2^i}\sum_{k=0}^{[i/2]}\dfrac{(-1)^{i-k+1}(2i-2k)!}{k!(i-k)!(i-2k+1)!} \\ \times\left[(\cos\theta_0)^{i-2k+1}-1\right](-1)^{n-i+m'}\sqrt{2n'+1}\begin{pmatrix} n & i & n' \\ m' & 0 & -m' \end{pmatrix} \end{array} \right\} \quad (36)$$

$$\Xi_1(n',n,\theta_0,m') = \varepsilon\sqrt{\pi}\sum_{\substack{i=|n'-n| \\ i-n'+n=\text{even}}}^{n+n'} \left\{ \begin{array}{l} \dfrac{\sqrt{2i+1}}{2^i}\sum_{k=0}^{[i/2]}\dfrac{(-1)^{i-k+1}(2i-2k)!}{k!(i-k)!(i-2k+1)!}\left[(\cos\theta_0)^{i-2k+1}-1\right] \\ \times\dfrac{1}{2}\left(\sqrt{\dfrac{n(n+1)}{n'(n'+1)}}+\sqrt{\dfrac{n'(n'+1)}{n(n+1)}}-\dfrac{i(i-1)}{\sqrt{n(n+1)n'(n'+1)}}\right) \\ \times(-1)^{n-i+m'}\sqrt{2n'+1}\begin{pmatrix} n & i & n \\ m' & 0 & -m' \end{pmatrix} \end{array} \right\} \quad (37)$$

and

$$\begin{pmatrix} n & i & n' \\ m' & 0 & -m' \end{pmatrix} =$$

$$= \left[\frac{(n+i-n')!(n-i+n')!(-n+i+n')!}{(n+i+n'+1)!}\right]^{1/2}\left[(n+m')!(n-m)!(i!)^2(n'-m')!(n'+m')!\right]^{1/2}\cdot$$

$$\times\sum_{z\in L}\frac{(-1)^{z+n+i+m'}}{z!(n+i+n'-z)!(n-m'-z)!(i-z)!(n'-i+m'+z)!(n'-n+z)!}$$

All the quantities $A, B, C, ...$ are given in Appendix A.

The algebraic equations (29) - (35) consist of a linear system of the following form

$$\boldsymbol{Dx} = \boldsymbol{0} \quad (38)$$

where

$$D=\begin{bmatrix} \boldsymbol{D}_{|m'|,|m'|} & \boldsymbol{D}_{|m'|,|m'|+1} & \boldsymbol{D}_{|m'|,|m'|+2} & \cdots & \cdots \\ \boldsymbol{D}_{|m'|+1,|m'|} & \boldsymbol{D}_{|m'|+1,|m'|+1} & \boldsymbol{D}_{|m'|+1,|m'|+2} & \cdots & \cdots \\ \boldsymbol{D}_{|m'|+2,|m'|} & \boldsymbol{D}_{|m'|+2,|m'|+1} & \boldsymbol{D}_{|m'|+2,|m'|+2} & \cdots & \cdots \\ \cdots & \cdots & \cdots & \cdots & \cdots \\ \cdots & \cdots & \cdots & \cdots & \cdots \end{bmatrix} \tag{39}$$

is a $7(n'+1)$ matrix (where n' ensures convergence)

and

$$\boldsymbol{x}=\left[\alpha_{|m'|}^{m',1},\alpha_{|m'|}^{m',2},\ldots,\gamma_{|m'|}^{m',2},-ic_{|m'|}^{m'},\ldots,-ic_{|m'|+1}^{m'},\ldots\right]^{T}.$$

Details about the matrix $\boldsymbol{D}$ are given in Appendix B.

In order for the system (38) to have non - trivial solutions, the frequency equation must be satisfied, that is

$$\det(\boldsymbol{D})=0. \tag{40}$$

Thus the equation (40) is going to provide with the complex eigenfrequencies $\Omega=\Omega_1+i\Omega_2$. At this point we note that matrix $\boldsymbol{D}$ is a complex matrix having as elements very complicated quantities constituted by combinations of Bessel functions having as argument the complex eigenfrequency Ω as well as the complicated complex quantities Ξ and Ξ_1. The numerical treatment of the matrix, as will be presented in section 5, requires the determination of the real and imaginary part of the matrix. To

fulfill this requirement we introduce the real quantities $\hat{\Xi}$ and $\hat{\Xi}_1$, which are defined by the equations

$$\Xi(n',n,\theta_0,m') = \varepsilon_1\hat{\Xi}(n',n,\theta_0,m') + i\varepsilon_2\hat{\Xi}(n',n,\theta_0,m') \tag{41}$$

$$\Xi_1(n',n,\theta_0,m') = \varepsilon_1\hat{\Xi}_1(n',n,\theta_0,m') + i\varepsilon_2\hat{\Xi}_1(n',n,\theta_0,m'). \tag{42}$$

The determination, now, of the real and imaginary part of the matrix is realised as follows: let us consider, for example, the (3,1) element of matrix $\boldsymbol{D}_{k,k}$, which has the following form:

$$d_{3,1} = A_k^1(r'_1) - \hat{A}_k^1(r'_1)\Xi(k,k,\theta_0,m').$$

By using the definition (41) we get

$$\begin{aligned} d_{3,1} = &\left\{\mathrm{Re}\,A_k^1(r'_1) - \left[\varepsilon_1\,\mathrm{Re}\,\hat{A}_k^1(r'_1) - \varepsilon_2\,\mathrm{Im}\,\hat{A}_k^1(r'_1)\right]\hat{\Xi}(k,k,\theta_0,m')\right\} \\ &+i\left\{\mathrm{Im}\,A_k^1(r'_1) - \left[\varepsilon_1\,\mathrm{Im}\,\hat{A}_k^1(r'_1) + \varepsilon_2\,\mathrm{Re}\,\hat{A}_k^1(r'_1)\right]\hat{\Xi}(k,k,\theta_0,m')\right\}. \end{aligned} \tag{43}$$

However, we have separated real from imaginary part just formally. The determination of $\mathrm{Re}\,A_k^1(r'_1)$ and $\mathrm{Im}\,A_k^1(r'_1)$ requires some analytical manipulations as well as use of suitable numerical schemes for the determination of the real and imaginary part of Spherical Bessel functions with complex argument. This procedure is repeated for every element of the truncated matrix $\boldsymbol{D}$.

4. Description of the Neck Support

The treatment of the neck support in the analysis described above is based on a complex variable $\varepsilon = \varepsilon_1 + i\varepsilon_2$ which depends on the mechanical properties of the neck. There is

no previous attempt in the literature to use such a model representing the neck with three - dimensional support elements. Landkof et al. [7] have used one support element which acts in one direction. In order to determine the most suitable model simulating neck support, we have considered many cases constituting combinations of Maxwell, Voight and Jeffrey elements [16]. Most of these models lead to non acceptable physically situations (negative parameters or values beyond the physically imposed constraints). Some complicated models having an extremely high degree of complexity do not provide with more information than simpler ones. All this analysis confined our choices to the selection of several, continuously and uniformly distributed model elements on the outer surface S_1 in three dimensions, each one of which has the structure shown in Fig. 2.

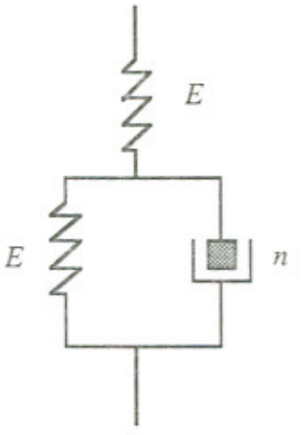

Figure 2: The Three Element Elastic Model.

It can easily be shown [14,15] for such a model that

$$\varepsilon = \frac{-i\Omega E\eta + E^2}{-i\Omega\eta + 2E}$$

or

$$\varepsilon_1 = \frac{E}{(2E+\eta\Omega_2)^2 + \eta^2\Omega_1^2}\left((E+\eta\Omega_2)(2E+\eta\Omega_2) + n^2\Omega_1^2\right)$$

and

$$\varepsilon_2 = -\frac{E}{(2E+\eta\Omega_2)^2+\eta^2\Omega_1^2}\eta\Omega_1 E,$$

where E,η dimensionless parameters ($E = E_s/\mu$, $\eta = \eta_s c_p/\mu\alpha$) and E_s, η_s the constants of the model of Fig. 2.

The determination of the parameters E,η is based on the agreement of (Ω_1, Ω_2) obtained by using our model and those of the experimental measurements of eigenfrequencies and damping coefficients. One particular set of data is of interest, whose parameters are given in Table 1 and concern the second fundamental eigenfrequency of the human head - neck system. The results obtained are shown in Table 1 and graphically in Figure 3. It is noticeable that the estimated parameters E,η of our model adapting the experimental data concerning the second basic eigenfrequency lead to a model reconstructing higher eigefrequencies in good agreement with experiment. This is the first necessary test for the acceptance of the specific parameter estimation.

Table 1: Parameters for the Three - Element Elastic Model Obtained from the second Eigenfrequency Experimental Data [2].

Experiment [2]		Constants fitted to Data	
$\omega_1^{(2)}$ (Hz)	$\omega_2^{(2)}$ (Hz)	E	n
1082	49.2	0.071	2.76
1378	49.2	0.077	0.95
1378	127.9	0.116	4.55
1082	127.9	0.121	1.66
Average		0.100	2.48

Figure 3: Model constants $\varepsilon_1, \varepsilon_2$ as a function of Ω_1, Ω_2 for average pairs E,n shown in Table 1.

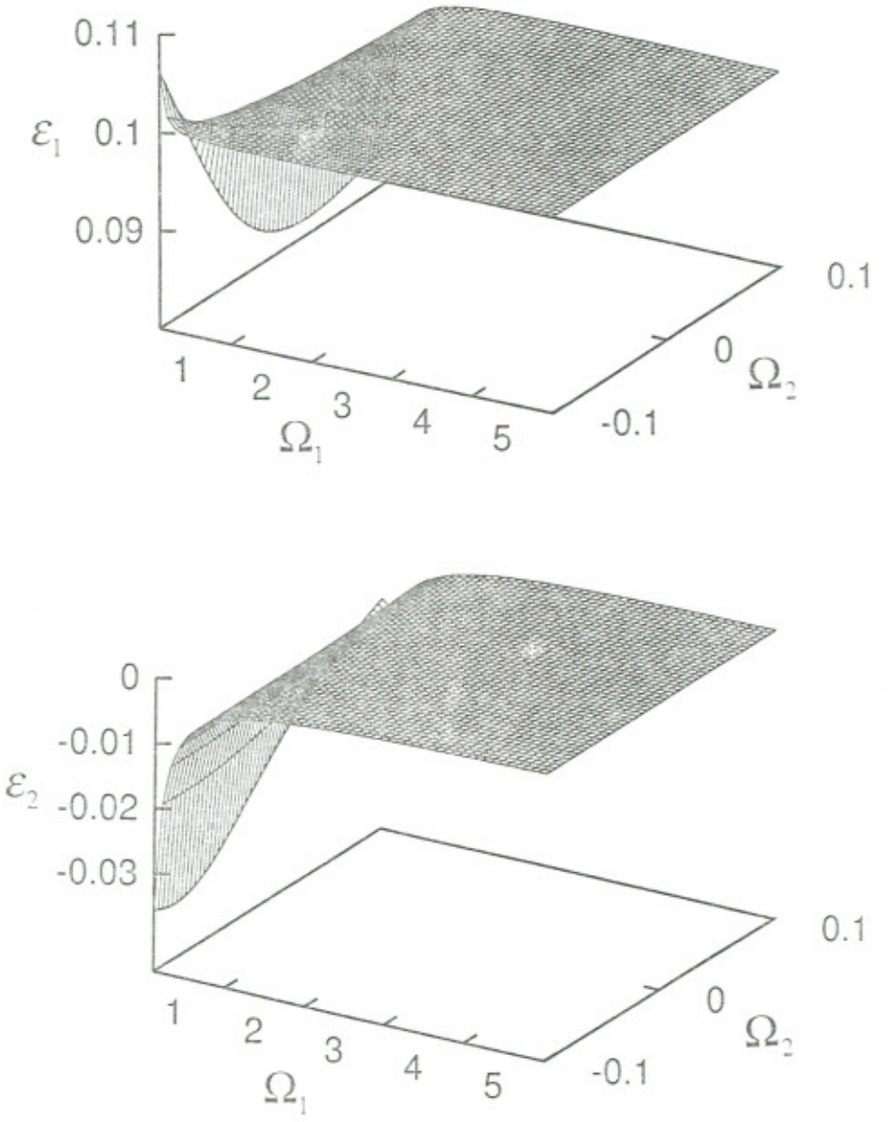

5. Numerical Results

The properties used for skull, brain and cerebrospinal fluid are given in Ref. 1. The geometry of the system is described by the following

$$r_1 = 0.0854m, \quad r_0 = 0.0794m, \quad \theta_0 = \frac{\pi}{8}$$

that reflects average geometrical characteristics of the experiments in Ref. 2.

The numerical method used is similar to the one described in Ref. 4. The dimension of the truncated matrix depends on the appropriate selection of the value of n' which ensures convergence of $\Omega^{(k)} = \Omega_1^{(k)} + i\Omega_2^{(k)}$, $k = 1,2,3,...,20$. The computation of $\Omega_1^{(k)}$ and $\Omega_2^{(k)}$ are listed in Tables 2 and 3, respectively. The results obtained are shown as a function of n' and in what follows we repeat the procedure until $\left\|\Omega^{(k)}(\varepsilon,\theta_o,n') - \Omega^{(k)}(\varepsilon,\theta_o,n'+1)\right\| \approx O(10^{-4})$, $k = 1,2,...,20$. As it is shown we obtain convergence of the first 11 eigenfrequencies for $n' = 1$. Using higher values of n' does not contribute to better predictions, although more eigenfrequencies can be computed, and makes the computations very intensive.

In Table 4 are cited experimental results [2] and the corresponding numerical results of our analysis. It is obvious that the results obtained using the constants computed above show very good agreement for the real part of the eigefrequencies. However, the first eigenfrequency cannot be predicted and this might be due to the complicated nature of the neck support of the human head. The first two computed damping coefficients fall within the region of the measured ones, and the viscoelastic behavior of the human neck does contribute significantly to higher damping coefficients. This shows that the viscoelastic behavior shown in the experimental results of Ref. 2 is mainly due to the viscoelastic properties of the human cavity.

The damping coefficients obtained by our analysis, the experimental ones and those obtained from a model for the viscoelastic brain [4] are shown in Table 5. The results

show that the first two of them are predicted by the present model and are not affected by the viscoelasticity of the human head and higher ones (9th and 10th) are predicted by the viscoelastic brain model. This indicates that the dynamic characteristics of the human head - system can only be predicted by a detailed model which incorporates both origins of viscous properties.

Another parameter which affects the obtained results is the support angle θ_0. The computed results for eigenfrequencies and damping coefficients is shown in Table 6.

6. Conclusions

In this work we have introduced a model for the simulation of the human head neck support which describes its viscoelastic properties. The parameters involved in the model have been computed using fitting to experimental dynamic characteristics. We assumed also that we can describe the human head using a simplified spherical cavity. Our results show that we can predict the real part of the eigefrequencies and the damping coefficients of the first two eigenfrequencies, being the only ones which are affected by the neck viscoelastic properties. However, the real part of the first eigenfrequency, which is important in certain clinical methods for the early diagnosis of brain diseases cannot be predicted by the proposed model and further investigation is needed.

Table 2: *Model convergence of* $\Omega_1^{(k)}$, $k = 1,2,...,19$.

No.	$n'=0$	$n'=1$	$n'=2$	$n'=3$	$n'=4$	$n'=5$	$n'=6$	$n'=7$	$n'=8$	$n'=9$
1		0.14174	0.14730	0.14551	0.14626	0.14592	0.14608	0.14601	0.14604	0.14602
2		0.34332	0.36101	0.35504	0.35756	0.35648	0.35691	0.35677	0.35680	0.35680
3			0.41568	0.42013	0.41834	0.41899	0.41881	0.41884	0.41884	0.41804
4				0.51837	0.51896	0.51837	0.51885	0.51852	0.51871	0.51861
5					0.62570	0.62722	0.62677	0.62694	0.62688	0.62690
6						0.73425	0.73611	0.73525	0.73568	0.73548
7							0.86501	0.86532	0.86513	0.86526
8								1.04509	1.04579	1.04548
9			1.18281	1.18281	1.18278	1.18283	1.18278	1.18283	1.18279	1.18281
10		1.19711	1.19823	1.19780	1.19802	1.19791	1.19795	1.19795	1.19797	1.19797
11									1.25233	1.25267
12										1.50691
13				1.90808	1.90867	1.90839	1.90846	1.90843	1.90844	1.90844
14			2.23668	2.23668	2.23667	2.23668	2.23667	2.23669	2.23668	2.23668
15	2.33386	2.33389	2.33389	2.33387	2.33390	2.33388	2.33389	2.33388	2.33389	2.33389
16					2.54067	2.54081	2.54071	2.54078	2.54074	2.54076
17						3.16689	3.16694	3.16691	3.16693	3.16692
18		3.24163	3.24162	3.24131	3.24131	3.24131	3.24131	3.24131	3.24131	3.24131
19				3.25936	3.25946	3.25942	3.25944	3.25943	3.25943	3.25943

Table 3: *Model convergence of* $\Omega_2^{(k)}$, $k = 1,2,...,19$.

No.	$n'=0$	$n'=1$	$n'=2$	$n'=3$	$n'=4$	$n'=5$	$n'=6$	$n'=7$	$n'=8$	$n'=9$
1		0.01724	0.01874	0.01838	0.01851	0.01846	0.01848	0.01847	0.01847	0.01847
2		0.01987	0.02205	0.02142	0.02167	0.02157	0.02161	0.02160	0.02160	0.02160
3			0.00145	0.00231	0.00204	0.00210	0.00210	0.00209	0.00209	0.00210
4				0.00021	0.00017	0.00023	0.00017	0.00021	0.00019	0.00020
5					0.00075	0.00095	0.00091	0.00092	0.00092	0.00092
6						0.00050	0.00069	0.00061	0.00065	0.00063
7							0.00010	0.00012	0.00011	0.00012
8								0.00041	0.00047	0.00044
9			0.00063	0.00063	0.00064	0.00063	0.00064	0.00063	0.00064	0.00063
10		0.00133	0.00141	0.00138	0.00139	0.00139	0.00139	0.00139	0.00139	0.00139
11									0.00150	0.00017
12										0.00014
13				0.00040	0.00042	0.00041	0.00042	0.00042	0.00042	0.00042
14			0.00009	0.00009	0.00009	0.00009	0.00009	0.00009	0.00009	0.00009
15	0.00007	0.00007	0.00007	0.00007	0.00007	0.00007	0.00007	0.00007	0.00007	0.00007
16					0.00007	0.00007	0.00007	0.00007	0.00007	0.00007
17						0.00005	0.00006	0.00006	0.00006	0.00005
18		0.00000	0.00000	0.00001	0.00001	0.00001	0.00001	0.00001	0.00001	0.00001
19				0.00012	0.00012	0.00012	0.00012	0.00012	0.00012	0.00012

Table 4: Comparison with Experimental Data [2].

No.	Experiment [2]		Present Analysis			
			First Set of Constants $E = 0.36,\ \eta = 7.98$		Second Set of Constants $E = 0.10,\ \eta = 2.48$	
	$\omega_1^{(i)}$ (Hz)	$\omega_2^{(i)}$ (Hz)	$\omega_1^{(i)}$ (Hz)	$\omega_2^{(i)}$ (Hz)	$\omega_1^{(i)}$ (Hz)	$\omega_2^{(i)}$ (Hz)
1	853-1091	49.6-123.4	1008.15	76.95	520.43	65.83
2	1082-1378	49.2-127.9	2468.17	39.81	1271.69	76.99
3	1373-1691	33.7-183.8	3693.02	104.36	1489.95	7.48
4	1616-1954	51.8-137.4	3882.56	12.01	1848.40	0.71
5	1859-2293	93.4-213.8	4478.31	1.20	2234.36	3.28
6	2084-2490	123.5-201.3	7024.64	8.42	2621.35	2.25
7	2260-2876	95.0-161.8	7899.56	2.82	3083.91	0.43
8	2510-3288	72.5-136.3	8357.55	1.07	3726.24	1.57
9	3213-3967	87.8-159.4	9073.48	1.85	4215.70	2.25
10	3558-4644	89.8-226.2	11332.40	0.99	4269.73	4.95
11	4197-5389	135.3-258.4	11543.18	0.19	4464.69	0.61
12	4644-5964	127.3-392.5	11717.36	2.04	5370.84	0.50

Table 5: Comparison of Damping Coefficients with Experimental Data [2] and Results from the Viscoelastic Brain Model [4].

No.	Experiment [2]	Present Analysis	Viscoelastic Brain Analysis [4]
1	49.6-123.4	65.83	
2	49.2-127.9	76.99	
3	33.7-183.8	7.48	6.196
4	51.8-137.4	0.71	12.799
5	93.4-213.8	3.28	18.314
6	123.5-201.3	2.25	23.161
7	95.0-161.8	0.43	27.669
8	72.5-136.3	1.57	32.017
9	87.8-159.4	2.25	130.788
10	89.8-226.2	4.95	97.095
11	135.3-258.4	0.61	36.265

Table 6: Variation of eigenfrequencies ($\omega_1^{(i)}$, $i = 1,...,10$) and damping coefficients ($\omega_2^{(i)}$, $i = 1,...,10$) v

$\theta_0 = \frac{\pi}{8}$		$\theta_0 = \frac{\pi}{15}$		$\theta_0 = \frac{\pi}{20}$	
$\omega_1^{(i)}$, $i = 1,...,12$	$\omega_2^{(i)}$, $i = 1,...,12$	$\omega_1^{(i)}$, $i = 1,...,12$	$\omega_2^{(i)}$, $i = 1,...,12$	$\omega_1^{(i)}$, $i = 1,...,12$	$\omega_2^{(i)}$, $i = 1,...,12$
520.43	65.83	252.75	51.08	176.44	36.87
1271.69	76.99	660.81	70.09	484.41	66.59
1489.95	7.48	1445.94	2.35	1436.08	1.31
1848.40	0.71	1836.68	0.65	1838.70	0.39
2234.36	3.28	2216.89	1.86	2206.97	1.12
2621.35	2.25	2575.46	0.38	2574.80	0.33
3083.91	0.43	3086.75	0.86	3082.38	0.62
3726.24	1.57	3691.74	0.09	3686.96	0.08
4215.70	2.25	4167.63	1.47	4149.27	0.83
4269.73	4.95	4242.12	0.69	4249.61	0.39

Acknowledgment

The present work forms part of the project "New Systems for Early Medical Diagnosis and Biotechnological Applications" which is supported by the Greek General Secretariat for Research and Technology through the EU funded R & D Program EPET II.

References

[1] Charalambopoulos A., Dassios G., Fotiadis D.I., and Massalas C.V.: Frequency Spectrum of the Human Head - Neck System, Int. J. Engng. Sci. 35(8) (1997) 753-768.

[2] Håkansson B., Brandt A. and Carlsson P.: Resonance Frequencies of the Human Skull *in vivo*, J. Acoust. Soc. Am. 95(3), (1994) 1474.

[3] Charalambopoulos A., Fotiadis D.I. and Massalas C.V.: Free Vibrations of the Viscoelastic Human Skull, Int. J. of Engng. Science, accepted (1997).

[4] Charalambopoulos A., Fotiadis D.I. and Massalas C.V.: The Effect of Viscoelastic Brain on the Dynamic Characteristics of the Human Skull - Brain System, Acta Mechanica, accepted (1997).

[5] McElhaney J.H., Fogle J.L., Melvin J.W., Haynes R.R., Roberts V.L. and Alem N.M.: Mechanical Properties of the Cranial Bone, J. of Biomechanics 3 (1970) 495 - 511.

[6] Schuck L.Z., Advani S.H.: Rheological Response of Human Brain Tissue in Shear, Transactions of the ASME, Journal of Basic Engineering, (1972) 905 - 911.

[7] Landkof B., Goldsmith W. and Sackman J.L.: Impact on a Head - Neck Structure, J. of Biomechanics 9 (1976) 141-151.

[8] Misra J.C. and Chakravarty S.: Dynamic Response of a Head - Neck System to an Impulsive Load, Mathematical Modelling 6 (1985) 83-96.

[9] Reber J.G. and Goldsmith W.: Analysis of Large Head - Neck Motions, J. Biomechanics 12 (1979) 211-222.

[10] Merrill T., Goldsmith W. and Deng Y.C.: Three - Dimensional Response of a Lumped Parameter Head - Neck Model due to Impact and Impulsive Loading, J. Biomechanics 17 (1984) 81-95.

[11] Langfitt T.W., Weinstein J.D. and Kassell N.F.: Vascular Factors in Head Injury: Contribution to Brain Swelling and Intracranial Hypertension. In Head Injury. Conference Proceedings, Chicago: Caveness W.F., and Walker J.B. (ed.), 172-194, Lippencott and Co., Philadelphia 1996.

[12] Huston R.L. and Seras J.: Effect of Protective Helmet Mass on Head/Neck Dynamics, Transactions of ASME 103 (1981) 18 - 23.

[13] Hansen W.W.: Phys. Rev. 47 (1935) 139.

[14] Bland D.R.: The Theory of Linear Viscoelasticity, Oxford, Pergamon Press, 1960.

[15] Christensen R.M.: Theory of Viscoelasticity: An Introduction, New York, Academic Press 1971.

[16] Joseph D.D.: Fluid Dynamics of Viscoelastic Fluids, New York, Springer - Verlag 1990.

APPENDIX A

The functions $A^l_{n',i}, B^l_{n',i}, C^l_{n',i}, D^l_{n',i}, E^l_{n',i}$ and $\hat{A}^l_{n'}, \hat{B}^l_{n'}, \hat{C}^l_{n'}, \hat{D}^l_{n'}, \hat{E}^l_{n'}$ are given as follows:

$$A^l_{n,i}(r') = -\left[\frac{4\mu'_i}{r'} g^l_n(k'_{p_i} r') + 2\mu'_i k'_{p_i}\left(1 - \frac{n(n+1)}{k'^2_{p_i} r'^2}\right) g^l_n(k'_{p_i} r') + \lambda'_i k'_{p_i} g^l_n(k'_{p_i} r')\right]$$

$$B^l_{n,i}(r') = 2\mu'_i \sqrt{n(n+1)}\left[\frac{1}{r'} \dot{g}^l_n(k'_{p_i} r') - \frac{g^l_n(k'_{p_i} r')}{k'_{p_i} r'^2}\right]$$

$$C^l_{n,i}(r') = \mu'_i \sqrt{n(n+1)}\left[k'_{s_i} \dot{g}^l_n(k'_{s_i} r') - \frac{1}{r'} g^l_n(k'_{s_i} r')\right]$$

$$D^l_{n,i}(r') = 2\mu'_i n(n+1)\left[\frac{\dot{g}^l_n(k'_{s_i} r')}{r'} - \frac{g^l_n(k'_{s_i} r')}{k'_{s_i} r'^2}\right]$$

$$E^l_{n,i}(r') = \mu'_i \sqrt{n(n+1)}\left[-2\frac{\dot{g}^l_n(k'_{s_i} r')}{r'} - k'_{s_i} g^l_n(k'_{s_i} r') + 2\frac{n(n+1)-1}{k'_{s_i} r'^2} g^l_n(k'_{s_i} r')\right]$$

$$\hat{A}^l_{n'} = g^l_{n'}(k'_p r')$$

$$\hat{B}^l_{n'} = \sqrt{n'(n'+1)}\frac{g^l_{n'}(k'_p r')}{k'_p r'}$$

$$\hat{C}^l_{n'} = \sqrt{n'(n'+1)} g^l_{n'}(k'_s r')$$

$$\hat{D}^l_{n'} = n'(n'+1)\frac{g^l_{n'}(k'_s r')}{k'_s r'}$$

$$\hat{E}^l_{n'} = \sqrt{n'(n'+1)}\left[\dot{g}^l_{n'}(k'_s r') + \frac{g^l_{n'}(k'_s r')}{k'_s r'}\right].$$

APPENDIX B

The matrix $\boldsymbol{D}$ can be described by a matrix of block elements having dimension 7 X 7, i.e.

$$\boldsymbol{D} = \begin{bmatrix} \boldsymbol{D}_{1,1} & \boldsymbol{D}_{1,2} & \cdots & \boldsymbol{D}_{1,n'+1} \\ \boldsymbol{D}_{2,1} & \cdots & \cdots & \cdots \\ \cdots & \cdots & \cdots & \cdots \\ \boldsymbol{D}_{n'+1,1} & \cdots & \cdots & \boldsymbol{D}_{n'+1,n'+1} \end{bmatrix}$$

The diagonal elements are given as

$$\boldsymbol{D} = \begin{bmatrix} d_{1,1} & d_{1,2} & \cdots & \cdots & \cdots & \cdots & d_{1,7} \\ d_{2,1} & \cdots & \cdots & \cdots & \cdots & \cdots & \cdots \\ \cdots & \cdots & \cdots & \cdots & \cdots & \cdots & \cdots \\ \cdots & \cdots & \cdots & \cdots & \cdots & \cdots & \cdots \\ \cdots & \cdots & \cdots & \cdots & \cdots & \cdots & \cdots \\ \cdots & \cdots & \cdots & \cdots & \cdots & \cdots & \cdots \\ d_{7,1} & \cdots & \cdots & \cdots & \cdots & \cdots & d_{7,7} \end{bmatrix}$$

where

$d_{1,1} = A_k^1(r'_0)$, $d_{1,2} = A_k^2(r'_0)$, $d_{1,5} = D_k^1(r'_0)$, $d_{1,6} = D_k^2(r'_0)$,

$d_{1,7} = -\dfrac{\Omega\rho'_f}{c'^2_s} g_k^1(k'_f r'_0)$,

$d_{2,1} = B_k^1(r'_0)$, $d_{2,2} = B_k^2(r'_0)$, $d_{2,5} = E_k^1(r'_0)$, $d_{2,6} = E_k^2(r'_0)$,

$d_{3,1} = A_k^1(r'_1) - \hat{A}_k^1(r'_1)\Xi(k,k,\theta_0,m')$, $d_{3,2} = A_k^2(r'_1) - \hat{A}_k^2(r'_1)\Xi(k,k,\theta_0,m')$,

$d_{3,5} = D_k^1(r'_1) - \hat{D}_k^1(r'_1)\Xi(k,k,\theta_0,m')$, $d_{3,6} = D_k^2(r'_1) - \hat{D}_k^2(r'_1)\Xi(k,k,\theta_0,m')$,

$d_{4,1} = B_k^1(r'_1) - \hat{B}_k^1(r'_1)\Xi(k,k,\theta_0,m')$, $d_{4,2} = B_k^2(r'_1) - \hat{B}_k^2(r'_1)\Xi(k,k,\theta_0,m')$,

$d_{4,5} = E_k^1(r'_1) - \hat{E}_k^1(r'_1)\Xi(k,k,\theta_0,m')$, $d_{4,6} = E_k^2(r'_1) - \hat{E}_k^2(r'_1)\Xi(k,k,\theta_0,m')$

$d_{5,3} = C_k^1(r'_0)$, $d_{5,4} = C_k^2(r'_0)$,

$$d_{6,3} = C_k^1(r'_1) - \hat{C}_k^1(r'_1)\Xi_1(k,k,\theta_0,m'), \quad d_{6,4} = C_k^2(r'_1) - \hat{C}_k^2(r'_1)\Xi_1(k,k,\theta_0,m')$$

$$d_{7,1} = \dot{g}_k^1(\Omega r'_0), \quad d_{7,2} = \dot{g}_k^2(\Omega r'_0), \quad d_{7,4} = k(k+1)\frac{g_k^1(k'_s r'_0)}{k'_s r'_0},$$

$$d_{7,5} = k(k+1)\frac{g_k^2(k'_s r'_0)}{k'_s r'_0}, \quad d_{7,7} = \frac{\dot{g}_k^1(k'_f r'_0)}{c'_f},$$

and the corresponding elements of the block submatrices $D_{k,j}$ are

$$d_{3,1} = -\hat{A}_j^1(r'_1)\Xi(k,j,\theta_0,m'), \quad d_{3,2} = -\hat{A}_j^2(r'_1)\Xi(k,j,\theta_0,m'),$$

$$d_{3,5} = -\hat{D}_j^1(r'_1)\Xi(k,j,\theta_0,m'), \quad d_{3,6} = -\hat{D}_j^2(r'_1)\Xi(k,j,\theta_0,m'),$$

$$d_{4,1} = -\hat{B}_j^1(r'_1)\Xi_1(k,j,\theta_0,m'), \quad d_{4,2} = -\hat{B}_j^2(r'_1)\Xi_1(k,j,\theta_0,m'),$$

$$d_{4,5} = -\hat{E}_j^1(r'_1)\Xi_1(k,j,\theta_0,m'), \quad d_{4,6} = -\hat{E}_j^2(r'_1)\Xi_1(k,j,\theta_0,m'),$$

$$d_{6,3} = -\hat{C}_j^1(r'_1)\Xi_1(k,j,\theta_0,m'), \quad d_{6,4} = -\hat{C}_j^2(r'_1)\Xi_1(k,j,\theta_0,m').$$